

# Vibration of a Bimodulus Thick Plate According to a Higher-Order Shear Deformation Theory

Ji-Liang Doong\* and Chin-Ping Fung†

National Central University, Taiwan, Republic of China

Equations of motion of a simply supported rectangular bimodulus thick plate in which the higher-order shear deformation terms are included are derived. The governing equations obtained using the average stress method are solved in exact form. The natural frequencies are compared with the previous results obtained for ordinary thick plates, and with the neutral surface locations and natural frequencies of bimodular plates. From those comparisons, the effects of higher-order shear deformation terms on the neutral surface locations and the natural frequencies can be observed. Also, the percentage error sense improvement by higher-order deformation terms can be reduced from 1.4 to 0.09%.

## Nomenclature

$a, b$	= dimensions of plate in $x, y$ directions
$A_{ij}, B_{ij}, D_{ij},$ $E_{ij}, F_{ij}, G_{ij},$ $H_{ij}$ $C_{ij}$	= laminate stiffness = components of the anisotropic stiffness matrix
$E^t, E^c$	= tensile and compressive Young's moduli, respectively
$G^t, G^c$	= tensile and compressive shear moduli, respectively
$h$	= plate thickness
$I_1, I_3, I_5, I_7$	= inertia coefficients of plate
$K$	= nondimensional buckling coefficient, $N_{xx}b^2/(\pi^2D_{22})$
$N_{xx}, M_{xx}, M_{xx}^*,$ $P_{xx}, P_{xx}^*, R_{xx},$ $R_{xx}^*$ $S$	= initial stress resultants = ratio of bending stress to normal stress, $\sigma_m/\sigma_n$
$u_x, u_y, w$	= displacement of plate ( $z = 0$ ) in $x, y, z$ directions
$\kappa^2$	= thickness-shear correction factor
$\nu^t, \nu^c$	= tensile and compressive Poisson's ratios, respectively
$\xi_x, \xi_y, \xi_z,$ $\phi_x, \phi_y$ $\rho$	= higher-order shear deformation term = density
$\sigma_{11}, \sigma_m, \sigma_n$	= initial, bending, and normal stress, respectively
$\bar{P}_i$	= applied surface traction
$\psi_x, \psi_y, \psi_z$	= rotations of plate in $x, y, z$ directions
$\Omega$	= nondimensional natural frequency, $\omega b^2/(\rho/E_{22}^c h^2)^{1/2}$
$\omega$	= neutral frequency

## Introduction

It is known that some composite materials behave differently in simple tension and compression.<sup>1</sup> In addition to composite materials, the tensile response of some polycrystalline graphites and high polymers also behave differently in tension and compression.<sup>2</sup> This characteristic behavior is actually curvilinear and is often approximated by two straight lines with a slope discontinuity at the origin. Thus, these materials are called bimodulus materials (see Fig. 1).

The bending and buckling of bimodulus-material plates have been the subject of a few studies.<sup>3-6</sup> The limited number of previous bimodulus-material-plate analyses are reviewed in Refs. 7-11; all were limited to static analyses. Bert et al.<sup>13</sup> and Bert and Kumar<sup>14</sup> are believed to be the first to study the vibration problem of thick bimodulus composite plates and shells. Doong and Chen<sup>15</sup> also studied the vibration problem of bimodulus plates in which the nonuniform initial stress is included.

Exact solutions for composite material structures have become available<sup>16,17</sup> and indicate that Mindlin-type theories (with five kinematic variables) do not adequately model the behavior of highly orthotropic composite structures. For improving the accuracy of Mindlin-type plate theories and keeping the advantages of two-dimensional problems, suitable higher-order plate theory is necessary. There are many theories of higher order<sup>18-21</sup> than that of the classical level that have been developed for use with composite plates. Probably the highest-order theory with 11 kinematic variables developed is by Lo et al.<sup>20</sup> A critical evaluation of new plate theories by Bert<sup>21</sup> indicated that the theory of Lo et al.<sup>20</sup> accurately predicted the nonlinear bending stress distribution.

In the present study, the previous work of Ref. 15 is extended to a higher-order bimodulus plate theory. The natural frequencies of a simply supported rectangular plate in a state of initial stress are presented. The natural frequencies obtained without initial stress for ordinary (not bimodulus) materials are compared with the exact solutions.<sup>17</sup> Also, the

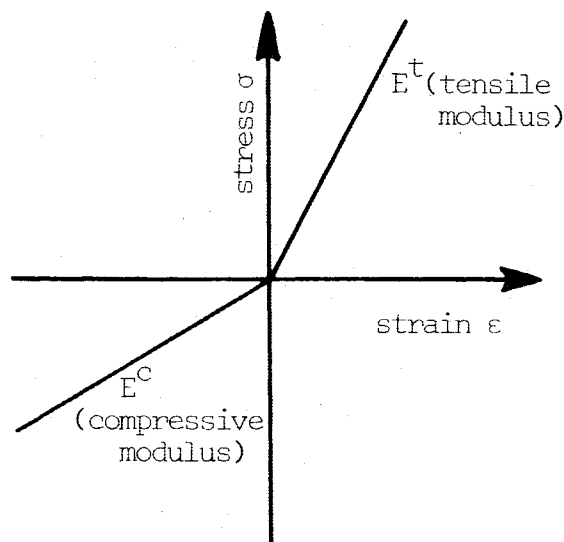


Fig. 1 Stress-strain relation of linearized different modulus material.

Received Dec. 11, 1986; revision received Aug. 14, 1987. Copyright © American Institute of Aeronautics and Astronautics, Inc., 1987. All rights reserved.

\*Associate Professor, Department of Mechanical Engineering.

†Graduate Student, Department of Mechanical Engineering.

neutral surface locations and natural frequencies of bimodulus plates are solved to compare with the results previously obtained by Doong and Chen<sup>15</sup> who studied the same problem by using Mindlin plate theory. The influences of various parameters on the vibration problems are investigated.

### Formulation

For bimodulus materials, the different properties in tension and compression cause a shift in the neutral surface away from the geometric midplane, and symmetry about the midplane no longer holds. The result of this is that bending-stretching couplings of an orthotropic type are exhibited, i.e., analogous to a two-layer crossply plate (one layer at 0 deg and the other at 90 deg) of ordinary orthotropic material. The governing equations of composite materials could be used for bimodulus materials, except that the stress-strain relation must be of the bimodulus form as shown in Appendix C. Doong<sup>22</sup> derived the governing equations based on a higher-order theory for a homogeneous plate in a general state of nonuniform initial stress. In previous work, the displacement field is chosen in a manner similar to that of Lo et al.<sup>20</sup> for homogeneous plates. We extend this class of theory to composite plates by using the average stress method outlined in Ref. 12.

We consider a simply supported rectangular bimodulus plate in a state of initial stress. The state of initial stress is

$$\sigma_{11} = \sigma_n + 2z\sigma_m/h \quad (1)$$

where  $\sigma_m$  and  $\sigma_n$  are taken to be constants and all other initial stresses are assumed to be zero. It is comprised of a tensile (compressive) plus a bending stress. The only nonzero stress and moment resultants are

$$N_{xx} = \int \sigma_{11} dz = h\sigma_n, \quad M_{xx} = \int \sigma_{11}z da = h^2\sigma_m/6$$

$$M_{xx}^* = \int \sigma_{11}z^2 dz = h^3\sigma_n/12$$

$$P_{xx} = \int \sigma_{11}z^3 dz = h^4\sigma_m/40, \quad P_{xx}^* = \int \sigma_{11}z^4 dz = h^5\sigma_n/80$$

$$R_{xx} = \int \sigma_{11}z^5 dz = h^6\sigma_m/224, \quad R_{xx}^* = \int \sigma_{11}z^6 dz = h^7\sigma_n/448 \quad (2)$$

where all the integrals are through the thickness of the plate from  $-h/2$  to  $h/2$ . Lateral loads and body forces are taken to be zero. For a crossply composite plate, the laminate stiffnesses consist of  $C_{16}$ ,  $C_{26}$ ,  $C_{36}$ ;  $C_{45}$  will be equal to zero (where  $C_{ij}$  are the stiffness coefficients of stress-strain relations). The governing equations and boundary conditions can be reduced from the previously derived governing equation.<sup>23</sup> They are as follows:

$$Q_{1,x} + Q_{2,y} + R_{1,x} = I_1 \ddot{u}_x + I_3 \ddot{\xi}_x \quad (3)$$

$$Q_{2,x} + Q_{3,y} + R_{9,x} = I_1 \ddot{u}_y + I_3 \ddot{\xi}_y \quad (4)$$

$$Q_{4,x} + Q_{5,y} + R_{30,x} = I_1 \ddot{w} + I_3 \ddot{\xi}_z \quad (5)$$

$$Q_{6,x} + Q_{7,y} - Q_4 + R_{2,x} = I_3 \ddot{\psi}_x + I_5 \ddot{\phi}_x \quad (6)$$

$$Q_{7,x} + Q_{8,y} - Q_5 + R_{10,x} = I_3 \ddot{\psi}_y + I_5 \ddot{\phi}_y \quad (7)$$

$$Q_{9,x} + Q_{10,y} - Q_{11} + R_{31,x} = I_3 \ddot{\psi}_z \quad (8)$$

$$Q_{12,x} + Q_{13,y} - 2Q_9 + R_{3,x} = I_3 \ddot{u}_x + I_5 \ddot{\xi}_x \quad (9)$$

$$Q_{13,x} + Q_{14,y} - 2Q_{10} + R_{11,x} = I_3 \ddot{u}_y + I_5 \ddot{\xi}_y \quad (10)$$

$$Q_{15,x} + Q_{16,y} - 2Q_{17} + R_{32,x} = I_3 \ddot{w} + I_5 \ddot{\xi}_z \quad (11)$$

$$Q_{18,x} + Q_{19,y} - 3Q_{15} + R_{4,x} = I_5 \ddot{\psi}_x + I_7 \ddot{\phi}_x \quad (12)$$

$$Q_{19,x} + Q_{20,y} - 3Q_{16} + R_{12,x} = I_5 \ddot{\psi}_y + I_7 \ddot{\phi}_y \quad (13)$$

where the defining equations for  $Q_1$ - $Q_{20}$  and  $R_1$ - $R_{32}$  are given in Appendix A. The first-order theory results based on Mindlin plate theory can be obtained by assuming  $\phi_x, \phi_y, \psi_z, \xi_y, \xi_x, \xi_z = 0$  and introducing the shear correction  $\kappa^2 (= 5/6)$  into  $A_{44}$  and  $A_{55}$ .

The boundary conditions are, for the simply supported plate, on the  $x = \text{const}$  edges

$$\begin{aligned} u_y = 0, \quad \psi_y = 0, \quad \xi_y = 0, \quad \phi_y = 0, \quad w = 0, \quad \psi_z = 0 \\ \xi_z = 0, \quad \bar{F}_{xx} + \Delta F_{xx} = Q_1 + R_1, \quad \bar{M}_{xx} + \Delta M_{xx} = Q_6 + R_2 \\ \bar{M}_{xx}^* + \Delta M_{xx}^* = Q_{12} + R_3, \quad \bar{P}_{xx} + \Delta P_{xx} = Q_{18} + R_4 \end{aligned} \quad (14)$$

and on the  $y = \text{const}$  edges

$$\begin{aligned} u_x = 0, \quad \psi_x = 0, \quad \xi_x = 0, \quad \phi_x = 0 \\ w = 0, \quad \psi_z = 0, \quad \xi_z = 0 \\ \bar{F}_{yy} + \Delta F_{yy} = Q_3, \quad \bar{M}_{yy} + \Delta M_{yy} = Q_8 \\ \bar{M}_{yy}^* + \Delta M_{yy}^* = Q_{14}, \quad \bar{P}_{yy} + \Delta P_{yy} = Q_{20} \end{aligned} \quad (15)$$

where

$$(\bar{F}_{ii}, \bar{M}_{ii}, \bar{M}_{ii}^*, \bar{P}_{ii}) = [\bar{P}_i(1, z, z^2, z^3) dz \quad (i = x, y)$$

$$(\Delta F_{ii}, \Delta M_{ii}, \Delta M_{ii}^*, \Delta P_{ii}) = [\Delta P_i(1, z, z^2, z^3) dz \quad (i = x, y)$$

and  $\bar{P}_i$  is the applied surface traction used in Ref. 23.

The governing equations and the boundary conditions are exactly satisfied in closed form by the following set of functions:

$$\begin{aligned} u_x, \psi_x, \xi_x, \phi_x = \Sigma \Sigma [h U_{mn}, \Psi_{xmn}(\xi_{xmn}/h), (\Phi_{xmn}/h^2)] \\ \times \cos(m\pi x/a) \sin(n\pi y/b) \cdot e^{i\omega_{mn}t} \\ u_y, \psi_y, \xi_y, \phi_y = \Sigma \Sigma [h V_{mn}, \Psi_{ymn}, (\xi_{ymn}/h), (\Phi_{ymn}/h^2)] \\ \times \sin(m\pi x/a) \cos(n\pi y/b) \cdot e^{i\omega_{mn}t} \\ w, \psi_z, \xi_z = \Sigma \Sigma [h W_{mn}, \Psi_{zmn}, (\xi_{zmn}/h)] \\ \times \sin(m\pi x/a) \sin(n\pi y/b) e^{i\omega_{mn}t} \end{aligned} \quad (16)$$

Substituting Eq. (16) into the governing equations (3-13) leads to the following  $11 \times 11$  symmetric matrix:

$$([C] - \lambda[G])[\Delta] = \{0\} \quad (17)$$

where

$$[\Delta] = \{U_{mn}, V_{mn}, W_{mn}, \Psi_{xmn}, \Psi_{ymn}, \Psi_{zmn}, \xi_{xmn}, \xi_{ymn}, \xi_{zmn}, \Phi_{xmn}, \Phi_{ymn}\}^T$$

The elements of the symmetric coefficient matrices  $[C]$  and  $[G]$  are given in Appendix B.

The in-plane compressive stress is contained in the buckling coefficient  $K$ . The in-plane bending stress is contained in the ratio of bending stress to normal stress  $S$ . Since the equations are homogeneous, the determinant of the coefficient matrix must vanish. This, in turn, leads to the eigenvalue problem for the determination of the natural frequencies.

To determine the position of the neutral surface, one sets the strain in the  $X$  direction,  $\epsilon_1$ , equal to zero

$$\epsilon_1 = u_{x,x} + z\psi_{x,x} + z^2\xi_{x,x} + z^3\phi_{x,x} = 0$$

**Table 1 Comparison of nondimensional natural frequency coefficient of ordinary plates between present solutions and exact solutions**  
 $(\Omega = \omega h / \sqrt{\rho/G}, a/b = 1, b/h = 10, \nu = 0.3, K = 0, S = 0)$

$m$	$n$	Exact solution Ref. (17)	Present first-order solution	Percentage error	Present higher-order solution	Percentage error
1	1	0.0932	0.0930	0.20	0.0932	0.00
1	2	0.2226	0.2218	0.36	0.2226	0.00
1	3	0.4171	0.4144	0.64	0.4172	0.02
1	4		0.6508		0.6573	
1	5	0.9268	0.9152	1.25	0.9275	0.07
2	2	0.3421	0.3402	0.55	0.3421	0.00
2	3	0.5239	0.5197	0.80	0.5240	0.02
2	4	0.7511	0.7431	1.00	0.7515	0.05
2	5		0.9959		1.0102	
3	3	0.6889	0.6821	1.00	0.6892	0.04
3	4		0.8949		0.8992	
3	5		1.1237		1.1416	
4	4	1.0889	1.0735	1.40	1.0899	0.09
4	5		1.2908		1.3137	
5	5		1.4890		1.5185	

**Table 2 Values of fundamental frequency coefficient with the various values of  $E'/E^c$  ( $a/b = 1, b/h = 10, K = 0, \Omega = \omega b^2 / (\rho E_{22}^c h^2)^{1/2}, Z_n = (z_n/h)$ )**

$E'/E^c$	Nondimensional natural frequency $\Omega$		Neutral surface location $Z_n$	
	First-order solution	Higher-order solution	First-order solution	Higher-order solution
0.2	3.4387	3.4244	-0.1978	-0.2008
0.4	4.3250	4.3237	-0.1184	-0.1203
0.6	4.8863	4.8896	-0.0678	-0.0689
0.8	5.3016	5.3068	-0.0302	-0.0307
1.0	5.6337	5.6397	0.0	0.0
1.2	5.9126	5.9200	0.0255	0.0259
1.4	6.1553	6.1658	0.0478	0.0487
1.6	6.3724	6.3895	0.0678	0.0691
1.8	6.5709	6.6013	0.0862	0.0879
2.0	6.7557	6.8133	0.1034	0.1054

**Table 3 Values of fundamental frequency  $\Omega$  for various values of buckling coefficient  $K$  ( $E'/E^c = 0.2, S = 0, a/b = 1, b/h = 10$ )**

$K$	First-order solution ( $Z_n = -0.1978$ )	Higher-order solution ( $Z_n = -0.2008$ )
-2.3	0.8439	0.1634(0.7980) <sup>a</sup>
-2.2	1.0933	0.7317(1.0578)
-2.1	1.2956	1.0218(1.2653)
-2.0	1.4702	1.2461(1.4434)
-1.9	1.6263	1.4358(1.6017)
-1.8	1.7686	1.6032(1.7457)
-1.7	1.9003	1.7546(1.8788)
-1.6	1.0234	1.8941(2.0030)
-1.5	2.1395	2.0239(2.1199)
-1.0	2.6445	2.5767(2.6277)
-0.5	3.0674	3.0303(3.0521)
0.0	3.4387	3.4244(3.4244)
0.5	3.7737	3.7775(3.7599)
1.0	4.0812	4.1004(4.0679)
1.5	4.3672	4.3996(4.3542)
2.0	4.6355	4.6797(4.6227)

<sup>a</sup> $D_{22}$  is chosen as the same value as in first-order plate theory.

or

$$z_n = -(z_n^2 \dot{\Phi}_x / h + z_n^3 \Phi_x / h^2 + hU) / \Psi_x \quad (18)$$

The nondimensional neutral surface location  $Z_n$  is defined as

$$Z_n = z_n / h = -(Z_n^2 \dot{\Phi}_x + Z_n^3 \Phi_x + U) / \Psi_x \quad (19)$$

An iterative procedure is used to obtain the final displacement ratio and corresponding natural frequency.

## Results and Discussions

There are so many parameters that can be varied that it would be difficult to present results for all cases. Only a few typical cases will be selected for discussion. For verifying the accuracy of present higher-order theory, the comparison between exact solution<sup>17</sup> and present solutions of an ordinary plate is the first to be considered and is shown in Table 1. From Table 1, it can be concluded that the present higher-order theory results coincide with exact solutions very well, and the accuracy of present higher-order theory results is better than present first-order theory results.

Nondimensional coefficients have been used to obtain the results shown in Figs. 2-6 and Tables 1-5. In the computations,  $E^c = 1.0$ ,  $\nu^c = 0.2$ ,  $E'/E^c = 0.2$  to 2.0, and  $\nu'$  is given by the relation

$$\nu' = \nu^c E'/E^c$$

The shear moduli  $G^c$  and  $G'$  in the respective compressive and tensile regions are

$$G^c = E^c / 2(1 + \nu^c), \quad G' = E' / 2(1 + \nu')$$

The values of  $\Omega$  for various  $E'/E^c$  ratios are shown in Table 2, where  $b/h$ ,  $a/b$ , and  $K$  are equal to 10, 1, and 0, respectively. It can be seen that the natural frequencies will increase with the values of  $E'/E^c$ , and neutral surface locations of higher-order plate theory results are further away from the middle plane than those of first-order plate theory results. The higher-order plate theory result is lower than the first-order plate theory result when  $E'/E^c < 1.0$  and opposite effects are observed as  $E'/E^c > 1.0$ .

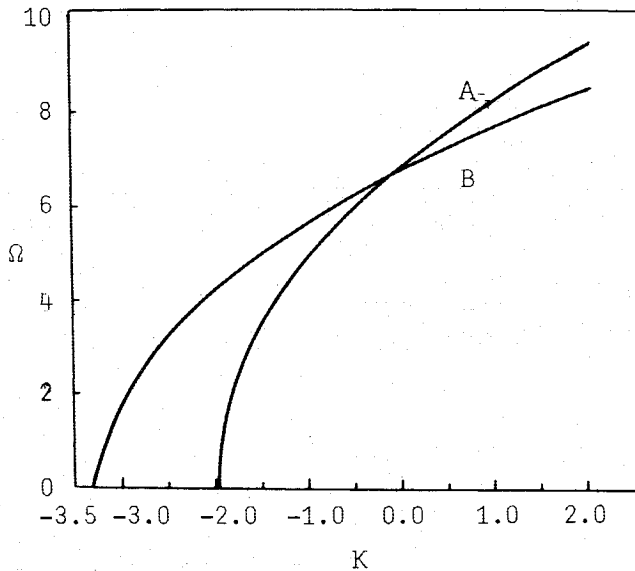


Fig. 2 Nondimensional frequency parameter  $\Omega$  vs buckling coefficient  $K$  for bimodulus plate  $A$ , higher-order theory result  $B$ , first-order theory result ( $E'/E^c = 2.0$ ,  $a/b = 1$ ,  $b/h = 10$ ,  $S = 0$ ).

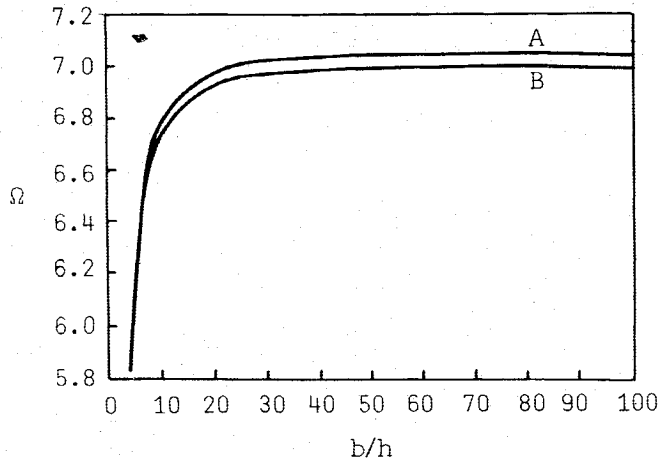


Fig. 3 Nondimensional frequency parameter  $\Omega$  vs thickness ratio  $b/h$  for bimodulus plate  $A$ , higher-order theory result  $B$ , first-order theory result ( $E'/E^c = 2.0$ ,  $a/b = 1$ ,  $K = 0$ ).

Table 4 Values of fundamental frequency  $\Omega$  for various values of buckling coefficient  $K$  ( $E'/E^c = 2.0$ ,  $S = 0$ ,  $a/b = 1$ ,  $b/h = 10$ )

$K$	First-order solution ( $Z_n = 0.1034$ )	Higher-order solution ( $Z_n = 0.1054$ )
-3.3	0.2493	(0.8449) <sup>a</sup>
-3.2	1.1501	(1.4488)
-3.1	1.6455	(1.8666)
-3.0	2.0230	(2.2066)
-2.5	3.3192	(3.4343)
-2.0	4.2357	(4.3266)
-1.9	4.3962	2.2331(4.4838)
-1.8	4.5510	2.6772(4.6357)
-1.7	4.7007	3.0575(4.7828)
-1.6	4.8457	3.3954(4.9254)
-1.5	4.9866	3.7027(5.0641)
-1.0	5.6383	4.9612(5.7070)
-0.5	6.2221	5.9596(6.2845)
0.0	6.7557	6.8133(6.8133)
0.5	7.2501	7.5713(7.3038)
1.0	7.7129	8.2600(7.7634)
1.5	8.1494	8.8956(8.1973)
2.0	8.5637	9.4887(8.6094)

<sup>a</sup> $D_{22}$  is chosen as the same value as in first-order plate theory.

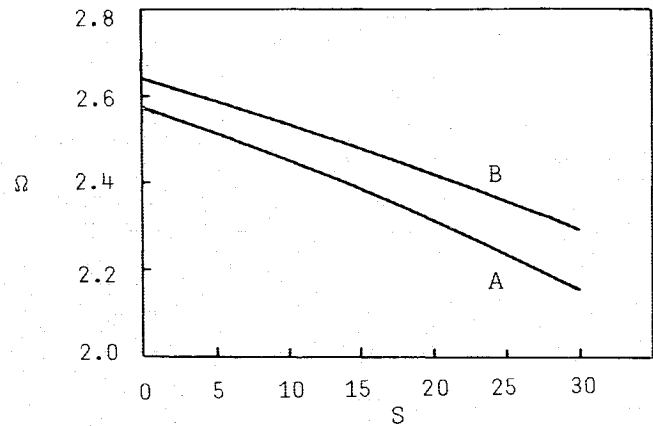


Fig. 4 Nondimensional frequency parameter  $\Omega$  vs bending stress ratio  $S$  for bimodulus plate  $A$ , higher-order theory result  $B$ , first-order theory result ( $E'/E^c = 0.2$ ,  $a/b = 1$ ,  $b/h = 10$ ,  $K = -1$ ).

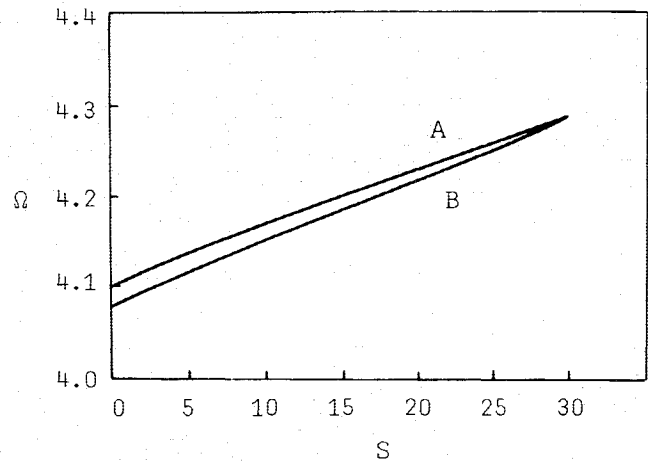


Fig. 5 Nondimensional frequency parameter  $\Omega$  vs bending stress ratio  $S$  for bimodulus plate  $A$ , higher-order theory result  $B$ , first-order theory result ( $E'/E^c = 0.2$ ,  $a/b = 1$ ,  $b/h = 10$ ,  $K = +1$ ).

The effect of initial stresses is studied in Tables 3 and 4. It is shown that the compressive stresses produce softening effects in the natural frequencies; the tensile stresses have reverse effects. The frequency will reduce to zero when the compressive stress increases. The buckling load is obtained when  $\Omega$  is zero (see Fig. 2). The significant difference of buckling loads between higher-order solution and first-order solution (also see Fig. 2) is due to the increasing of  $D_{22}$  in higher-order plate theory. If the same  $D_{22}$  values as in first-order plate theory are chosen to calculate the new nondimensional buckling coefficients, then closer results can be observed (see Tables 3 and 4). Plots of  $\Omega$  vs the thickness ratio  $b/h$  are given in Fig. 3. Owing to the nondimensional coefficient effect, the nondimensional frequencies  $\Omega$  increase with the increase of thickness ratio.

Plots of nondimensional frequency coefficient  $\Omega$  vs the ratio of bending stress to normal stress  $S$  are made in Figs. 4 and 5.  $b/h$ ,  $a/b$ , and  $E'/E^c$  are equal to 10, 1, and 0.2 in that order the  $K$  is equal to  $-1$  and  $+1$ , respectively. The bending stress effects are shown to reduce the frequencies significantly when  $K$  is negative and  $S$  is positive. If  $K$  and  $S$  are positive, then the opposite results are obtained. For ordinary plates, the effects of bending stress are shown in Fig. 6. It can be seen that the bending stress has little effect on the natural frequency. This conclusion agrees with the results of Brunelle and Robertson<sup>24</sup> and the previous results of the present authors.<sup>22,23</sup> The effect of the aspect ratio on frequency is given in Table 5, where  $b/h$ ,  $E'/E^c$ ,  $K$ , and  $S$  are equal to 10, 0.2–2.0, 0, and 0, respectively. It is seen that the larger the aspect ratio  $a/b$ , the lower the frequency coefficient.

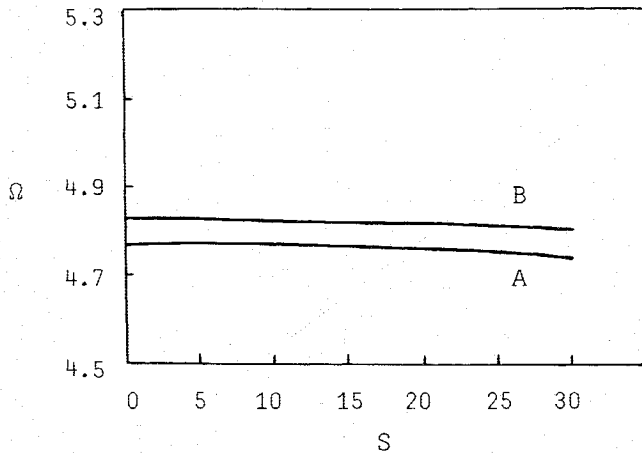


Fig. 6 Nondimensional frequency parameter  $\Omega$  vs bending stress ratio  $S$  for ordinary plate  $A$ , higher-order theory result  $B$ , first-order theory result ( $E'/E^c = 1.0$ ,  $a/b = 1$ ,  $b/h = 10$ ,  $K = -1$ ,  $\nu = 0.2$ ).

Table 5 Values of fundamental frequency  $\Omega$  for various values of aspect ratio  $a/b$  ( $b/h = 10$ ,  $K = 0$ )

$a/b$	$E'/E^c = 0.2$		$E'/E^c = 2.0$	
	First-order solution	Higher-order solution	First-order solution	Higher-order solution
0.4	11.6170	11.4275	22.5995	22.7689
0.6	6.3329	6.2788	12.3948	12.5035
0.8	4.3699	4.3455	8.5743	8.6483
1.0	3.4387	3.4244	6.7557	6.8133
1.2	2.9266	2.9167	5.7536	5.8022
1.6	2.4128	2.4066	4.7469	4.7867
2.0	2.1734	2.1686	4.2774	4.3131
2.4	2.0430	2.0389	4.0215	4.0549
2.8	1.9642	1.9605	3.8668	3.8989
3.2	1.9130	1.9095	3.7662	3.7975
3.6	1.8778	1.8745	3.6973	3.7279
4.0	1.8527	1.8495	3.6479	3.6781

### Conclusions

The preliminary results indicate the following:

- 1) Using the present higher-order plate theory, one can obtain the same results as with the exact solutions and the accuracy of the present higher-order plate theory is better than that of the first-order plate theory.
- 2) The influences of higher-order shear deformation displacements on the natural frequency  $\Omega$  for bimodulus plates are lower in value when  $E'/E^c < 1.0$  and opposite effects are observed as  $E'/E^c > 1.0$ .
- 3) The nondimensional frequency  $\Omega$  increases with increasing  $E'/E^c$ .
- 4) The initial compressive stresses significantly reduce the frequency; the tensile stresses have the reverse effect.
- 5) The frequency decreases significantly with the increase of an initial bending stress coefficient for a bimodulus plate, when  $K$  is negative.  $S$  has little effect on  $\Omega$  for an ordinary plate.
- 6) The thicker the plate, the lower the nondimensional frequency  $\Omega$ . The natural frequencies  $\omega$  of thick plates are larger than those of thin plates.
- 7) Nondimensional frequency decreases with aspect ratio  $a/b$ .

### Appendix A: Defining Equations for

$Q_1 - Q_{20}$  and  $R_1 - R_{32}$  in Eqs. (3)-(13)

$$Q_1 = A_{11}u_{x,x} + A_{12}u_{y,y} + A_{13}\psi_z + D_{11}\xi_{x,x} + D_{12}\xi_{y,y} + B_{11}\psi_{x,x} + B_{12}\psi_{y,y} + 2B_{13}\xi_z + E_{11}\phi_{x,x} + E_{12}\phi_{y,y}$$

$$Q_2 = A_{66}(u_{x,y} + u_{y,x}) + D_{66}(\xi_{x,y} + \xi_{y,x}) + B_{66}(\psi_{x,y} + \psi_{y,x}) + E_{66}(\phi_{x,y} + \phi_{y,x})$$

$$Q_3 = A_{12}u_{x,x} + A_{22}u_{y,y} + A_{23}\psi_z + D_{12}\xi_{x,x} + D_{22}\xi_{y,y} + B_{12}\psi_{x,x} + B_{22}\psi_{y,y} + 2B_{23}\xi_z + E_{12}\phi_{x,x} + E_{22}\phi_{y,y}$$

$$Q_4 = A_{55}(w_{,x} + \psi_x) + D_{55}(\xi_{z,x} + 3\phi_x) + B_{55}(2\xi_x + \psi_{z,x})$$

$$Q_5 = A_{44}(w_{,y} + \psi_y) + D_{44}(\xi_{z,y} + 3\phi_y) + B_{44}(2\xi_y + \psi_{z,y})$$

$$Q_6 = D_{11}\psi_{x,x} + D_{12}\psi_{y,y} + 2D_{13}\xi_z + F_{11}\phi_{x,x} + F_{12}\phi_{y,y} + B_{11}u_{x,x} + B_{12}u_{y,y} + B_{13}\psi_z + E_{11}\xi_{x,x} + E_{12}\xi_{y,y} + F_{11}\phi_{x,x} + F_{12}\phi_{y,y}$$

$$Q_7 = D_{66}(\psi_{x,y} + \psi_{y,x}) + F_{66}(\phi_{x,y} + \phi_{y,x}) + B_{66}(u_{x,y} + u_{y,x}) + E_{66}(\xi_{x,y} + \xi_{y,x})$$

$$Q_8 = D_{12}\psi_{x,x} + D_{22}\psi_{y,y} + 2D_{23}\xi_z + F_{12}\phi_{x,x} + F_{22}\phi_{y,y} + B_{12}u_{x,x} + B_{22}u_{y,y} + B_{23}\psi_z + E_{12}\xi_{x,x} + E_{22}\xi_{y,y}$$

$$Q_9 = D_{55}(2\xi_x + \psi_{z,x}) + B_{55}(\psi_x + w_{,x}) + E_{55}(3\phi_x + \xi_{z,x})$$

$$Q_{10} = D_{44}(2\xi_y + \psi_{z,y}) + B_{44}(\psi_y + w_{,y}) + E_{44}(3\phi_y + \xi_{z,y})$$

$$Q_{11} = A_{13}u_{x,x} + A_{23}u_{y,y} + A_{33}\psi_z + D_{13}\xi_{x,x} + D_{23}\xi_{y,y} + B_{13}\psi_{x,x} + B_{23}\psi_{y,y} + 2B_{33}\xi_z + E_{13}\phi_{x,x} + E_{23}\phi_{y,y}$$

$$Q_{12} = D_{11}u_{x,x} + D_{12}u_{y,y} + D_{13}\psi_z + F_{11}\xi_{x,x} + F_{12}\xi_{y,y} + E_{11}\psi_{x,x} + E_{12}\psi_{y,y} + 2E_{13}\xi_z + G_{11}\phi_{x,x} + G_{12}\phi_{y,y}$$

$$Q_{13} = D_{66}(u_{x,y} + u_{y,x}) + F_{66}(\xi_{x,y} + \xi_{y,x}) + E_{66}(\psi_{x,y} + \psi_{y,x}) + G_{66}(\phi_{x,y} + \phi_{y,x})$$

$$Q_{14} = D_{12}u_{x,x} + D_{22}u_{y,y} + D_{23}\psi_z + F_{12}\xi_{x,x} + F_{22}\xi_{y,y} + E_{12}\psi_{x,x} + E_{22}\psi_{y,y} + 2E_{23}\xi_z + G_{12}\phi_{x,x} + G_{22}\phi_{y,y}$$

$$Q_{15} = D_{55}(w_{,x} + \psi_x) + F_{55}(\xi_{z,x} + 3\phi_x) + E_{55}(2\xi_x + \psi_{z,x})$$

$$Q_{16} = D_{44}(w_{,y} + \psi_y) + F_{44}(\xi_{z,y} + 3\phi_y) + E_{44}(2\xi_y + \psi_{z,y})$$

$$Q_{17} = 2D_{33}\xi_z + D_{13}\psi_{x,x} + D_{23}\psi_{y,y} + F_{13}\phi_{x,x} + F_{23}\phi_{y,y} + B_{13}u_{x,x} + B_{23}u_{y,y} + B_{33}\psi_z + E_{23}\xi_{y,y} + E_{13}\xi_{x,x}$$

$$Q_{18} = F_{11}\psi_{x,x} + F_{12}\psi_{y,y} + 2F_{13}\xi_z + H_{11}\phi_{x,x} + H_{12}\phi_{y,y} + E_{11}u_{x,x} + E_{12}u_{y,y} + E_{13}\psi_z + G_{11}\xi_{x,x} + G_{12}\xi_{y,y}$$

$$Q_{19} = F_{66}(\psi_{x,y} + \psi_{y,x}) + H_{66}(\phi_{x,y} + \phi_{y,x}) + E_{66}(u_{x,y} + u_{y,x}) + G_{66}(\xi_{x,y} + \xi_{y,x})$$

$$Q_{20} = F_{12}\psi_{x,x} + F_{22}\psi_{y,y} + 2F_{23}\xi_z + H_{12}\phi_{x,x} + H_{22}\phi_{y,y} + E_{12}u_{x,x} + E_{22}u_{y,y} + E_{23}\psi_z + G_{12}\xi_{x,x} + G_{22}\xi_{y,y}$$

and

$$R_1 = N_{xx}u_{x,x} + M_{xx}\psi_{x,x} + M_{xx}^*\xi_{x,x} + P_{xx}\phi_{x,x}$$

$$R_2 = M_{xx}u_{x,x} + M_{xx}^*\psi_{x,x} + P_{xx}\xi_{x,x} + P_{xx}^*\phi_{x,x}$$

$$R_3 = M_{xx}^*u_{x,x} + P_{xx}\psi_{x,x} + P_{xx}^*\xi_{x,x} + R_{xx}\phi_{x,x}$$

$$\begin{aligned}
R_4 &= P_{xx}u_{x,x} + P_{xx}^*\psi_{x,x} + R_{xx}\xi_{x,x} + R_{xx}^*\phi_{x,x} \\
R_9 &= N_{xx}u_{y,x} + M_{xx}\psi_{y,x} + M_{xx}^*\xi_{y,x} + P_{xx}\phi_{y,x} \\
R_{10} &= M_{xx}u_{y,x} + M_{xx}^*\psi_{y,x} + P_{xx}\xi_{y,x} + P_{xx}^*\phi_{y,x} \\
R_{11} &= M_{xx}^*u_{y,x} + P_{xx}\psi_{y,x} + P_{xx}^*\xi_{y,x} + R_{xx}\phi_{y,x} \\
R_{12} &= P_{xx}u_{y,x} + P_{xx}^*\psi_{y,x} + R_{xx}\xi_{y,x} + R_{xx}^*\phi_{y,x} \\
R_{30} &= N_{xx}w_{x,x} + M_{xx}\psi_{z,x} + M_{xx}^*\xi_{z,x} \\
R_{31} &= M_{xx}w_{x,x} + M_{xx}^*\psi_{z,x} + P_{xx}\xi_{z,x} \\
R_{32} &= M_{xx}^*w_{x,x} + P_{xx}\psi_{z,x} + P_{xx}^*\xi_{z,x}
\end{aligned}$$

### Appendix B:

#### Coefficients of Matrix [C] and [G] in Eq. (17)

$$(\alpha = m\pi/a, \beta = n\pi/b)$$

$$\begin{aligned}
C_{1,1} &= -(A_{11} + N_{xx})\alpha^2 - A_{66}\beta^2 \\
C_{1,2} &= -(A_{12} + A_{66})\alpha\beta \\
C_{1,4} &= -(M_{xx}\alpha^2 + B_{66}\beta^2 + B_{11}\alpha^2)/h \\
C_{1,5} &= -(B_{12} + B_{66})\alpha\beta/h \\
C_{1,6} &= A_{13}\alpha/h \\
C_{1,7} &= [- (D_{11} + M_{xx}^*)\alpha^2 - D_{66}\beta^2]/h^2 \\
C_{1,8} &= -(D_{12} + D_{66})\alpha\beta/h^2 \\
C_{1,9} &= 2B_{13}\alpha/h^2 \\
C_{1,10} &= [-P_{xx}\alpha^2 - (E_{11}\alpha^2 + E_{66}\beta^2)]/h^3 \\
C_{1,11} &= -(E_{12} + E_{66})\alpha\beta/h^3 \\
C_{2,2} &= -A_{22}\beta^2 - (A_{66} + N_{xx})\alpha^2 \\
C_{2,4} &= C_{1,5} \\
C_{2,5} &= [-M_{xx}\alpha^2 - (B_{66}\alpha^2 + B_{22}\beta^2)]/h \\
C_{2,6} &= A_{23}\beta/h \\
C_{2,7} &= C_{1,8} \\
C_{2,8} &= [-D_{22}\beta^2 - (D_{66} + M_{xx}^*)\alpha^2]/h^2 \\
C_{2,9} &= 2B_{23}\beta/h^2 \\
C_{2,10} &= C_{1,11} \\
C_{2,11} &= [-P_{xx}\alpha^2 - (E_{66}\alpha^2 + E_{22}\beta^2)]/h^3 \\
C_{3,3} &= -(A_{55} + N_{xx})\alpha^2 - A_{44}\beta^2 \\
C_{3,4} &= -A_{55}\alpha/h \\
C_{3,5} &= -A_{44}\beta/h \\
C_{3,6} &= [-M_{xx}\alpha^2 - (B_{55}\alpha^2 + B_{44}\beta^2)]/h \\
C_{3,7} &= -2B_{55}\alpha/h^2 \\
C_{3,8} &= -2B_{44}\beta/h^2 \\
C_{3,9} &= -[(D_{55} + M_{xx}^*)\alpha^2 + D_{44}\beta^2]/h^2
\end{aligned}$$

$$\begin{aligned}
C_{3,10} &= -3D_{55}\alpha/h^3 \\
C_{3,11} &= -3D_{44}\beta/h^3 \\
C_{4,4} &= -[(D_{11} + M_{xx}^*)\alpha^2 + D_{66}\beta^2 + A_{55}]/h^2 \\
C_{4,5} &= C_{1,8} \\
C_{4,6} &= (B_{13} - B_{55})\alpha/h^2 \\
C_{4,7} &= [-P_{xx}\alpha^2 - (E_{11}\alpha^2 + E_{66}\beta^2 + 2B_{55})]/h^2 \\
C_{4,8} &= -(E_{12} + E_{66})\alpha\beta/h^3 \\
C_{4,9} &= (2D_{13} - D_{55})\alpha/h^3 \\
C_{4,10} &= -[(F_{11} + P_{xx}^*)\alpha + F_{66}\beta^2 - 3D_{55}]/h^4 \\
C_{4,11} &= -(F_{12} + F_{66})\alpha\beta/h \\
C_{5,5} &= [-D_{22}\beta^2 - (D_{66} + M_{xx}^*)\alpha^2 - A_{44}]/h^2 \\
C_{5,6} &= (B_{23} - B_{44})\beta/h^2 \\
C_{5,7} &= C_{4,8} \\
C_{5,8} &= [-P_{xx}\alpha^2 - (E_{66}\alpha^2 + E_{22}\beta^2) - 2B_{44}]/h^2 \\
C_{5,9} &= (2D_{23} - D_{44})\beta/h^3 \\
C_{5,10} &= -(F_{12} + F_{66})\alpha\beta/h^4 \\
C_{5,11} &= -[F_{22}\beta^2 + (F_{66} + P_{xx}^*)\alpha^2 + 3D_{44}]/h^4 \\
C_{6,6} &= -[(D_{55} + M_{xx}^*)\alpha^2 + D_{44}\beta^2 + A_{33}]/h^2 \\
C_{6,7} &= (-2D_{55} + D_{13})\alpha/h^3 \\
C_{6,8} &= (-2D_{44} + D_{23})\beta/h^3 \\
C_{6,9} &= [-P_{xx}\alpha^2 - (E_{55}\alpha^2 + E_{44}\beta^2) - 2B_{33}]/h^3 \\
C_{6,10} &= -(3E_{55} + E_{13})\alpha/h^4 \\
C_{6,11} &= -(3E_{44} + E_{23})\beta/h^4 \\
C_{7,7} &= -[(F_{11} + P_{xx}^*)\alpha^2 + F_{66}\beta^2 + 4D_{55}]/h^4 \\
C_{7,8} &= -(F_{12} + F_{66})\alpha\beta/h^4 \\
C_{7,9} &= (2E_{13} - 2E_{55})\alpha/h^4 \\
C_{7,10} &= [-R_{xx}\alpha^2 - (G_{11}\alpha^2 + G_{66}\beta^2) - 6E_{55}]/h^5 \\
C_{7,11} &= -(G_{12} + G_{66})\alpha\beta/h^5 \\
C_{8,8} &= -[F_{22}\beta^2 + (F_{66} + P_{xx}^*)\alpha^2 + 4D_{44}]/h^4 \\
C_{8,9} &= (2E_{23} - 2E_{44})\beta/h^4 \\
C_{8,10} &= C_{7,11} \\
C_{8,11} &= [-R_{xx}\alpha^2 - (G_{66}\alpha^2 + G_{22}\beta^2) - 6E_{44}]/h^5 \\
C_{9,9} &= -[(F_{55} + P_{xx}^*)\alpha^2 + F_{44}\beta^2 + 4D_{33}]/h^4 \\
C_{9,10} &= (-3F_{55} + 2F_{13})\alpha/h^5 \\
C_{9,11} &= (-3F_{44} + 2F_{23})\beta/h^5 \\
C_{10,10} &= -[(H_{11} + R_{xx}^*)\alpha^2 + H_{66}\beta^2 + 9F_{55}]/h^6 \\
C_{10,11} &= -(H_{12} + H_{66})\alpha\beta/h^6
\end{aligned}$$

$$C_{11,11} = -[(H_{66} + R_{xx}^*)\alpha^2 + H_{22}\beta^2 + 9F_{44}]/h^6$$

$$G_{1,1} = G_{2,2} = G_{3,3} = -I_1$$

$$G_{1,7} = G_{2,8} = G_{3,9} = G_{4,4} = G_{5,5} = G_{6,6} = -I_3/h^2$$

$$G_{4,10} = G_{5,11} = G_{7,7} = G_{8,8} = G_{9,9} = -I_5/h^4$$

$$G_{10,10} = G_{11,11} = -I_7/h^6$$

### Appendix C:

The generalized Hooke's law for stress-strain relations of an orthotropic bimodulus plate are given by

$$\begin{pmatrix} \sigma_x \\ \sigma_y \\ \sigma_z \\ \tau_{yz} \\ \tau_{zx} \\ \tau_{xy} \end{pmatrix} = \begin{pmatrix} C_{11k} & C_{12k} & C_{13k} & 0 & 0 & 0 \\ C_{12k} & C_{22k} & C_{23k} & 0 & 0 & 0 \\ C_{13k} & C_{23k} & C_{33k} & 0 & 0 & 0 \\ 0 & 0 & 0 & C_{44k} & 0 & 0 \\ 0 & 0 & 0 & 0 & C_{55k} & 0 \\ 0 & 0 & 0 & 0 & 0 & C_{66k} \end{pmatrix} \begin{pmatrix} \epsilon_x \\ \epsilon_y \\ \epsilon_z \\ \gamma_{yz} \\ \gamma_{zx} \\ \gamma_{xy} \end{pmatrix}$$

where  $C_{ij}$  are the stiffness coefficients of the stress-strain relations used in Ref. 25, and the third subscript ( $K$ ) refers to the sign of the strain ( $K = 1$  for tension and  $K = 2$  for compression). The general integral expressions for  $A_{ij}$ ,  $B_{ij}$ ,  $D_{ij}$ ,  $E_{ij}$ ,  $F_{ij}$ ,  $G_{ij}$ , and  $H_{ij}$  are for the portion (from  $Z = -h/2$  to  $Z = Zn$ ) in compression, whereas the upper portion is in tension

$$(A_{ij}, B_{ij}, D_{ij}, E_{ij}, F_{ij}, G_{ij}, H_{ij})$$

$$= \int_{-h/2}^{h/2} (C_{ij})(1, z, z^2, z^3, z^4, z^5, z^6), dz \quad i, j = 1, 2, 3, 4, 5, 6,$$

$$A_{ij} = \int_{-h/2}^{h/2} C_{ijk} dz$$

$$= \int_{-h/2}^{Z_n} C_{ij2} dz + \int_{Z_n}^{h/2} C_{ij1} dz$$

$$= h[(C_{ij2} + C_{ij1})/2 + (C_{ij2} - C_{ij1})Z_n]$$

$$B_{ij} = \int_{-h/2}^{h/2} C_{ijk} z dz$$

$$= \int_{-h/2}^{Z_n} C_{ij2} z dz + \int_{Z_n}^{h/2} C_{ij1} z dz$$

$$= h^2[(C_{ij1} - C_{ij2})/8 + (C_{ij2} - C_{ij1})(Z_n^2/2)]$$

$$D_{ij} = \int_{-h/2}^{h/2} C_{ijk} z^2 dz$$

$$= \int_{-h/2}^{Z_n} C_{ij2} z^2 dz + \int_{Z_n}^{h/2} C_{ij1} z^2 dz$$

$$= h^3[(C_{ij1} + C_{ij2})/24 + (C_{ij2} - C_{ij1})(Z_n^3/3)]$$

$$E_{ij} = \int_{-h/2}^{h/2} C_{ijk} z^3 dz$$

$$= \int_{-h/2}^{Z_n} C_{ij2} z^3 dz + \int_{Z_n}^{h/2} C_{ij1} z^3 dz$$

$$= h^4[(C_{ij1} - C_{ij2})/64 + (C_{ij2} - C_{ij1})(Z_n^4/4)]$$

$$F_{ij} = \int_{-h/2}^{h/2} C_{ijk} z^4 dz$$

$$= \int_{-h/2}^{Z_n} C_{ij2} z^4 dz + \int_{Z_n}^{h/2} C_{ij1} z^4 dz$$

$$= h^5[(C_{ij1} + C_{ij2})/160 + (C_{ij2} - C_{ij1})(Z_n^5/5)]$$

$$G_{ij} = \int_{-h/2}^{h/2} C_{ijk} z^5 dz$$

$$= \int_{-h/2}^{Z_n} C_{ij2} z^5 dz + \int_{Z_n}^{h/2} C_{ij1} z^5 dz$$

$$= h^6[(C_{ij1} - C_{ij2})/384 + (C_{ij2} - C_{ij1})(Z_n^6/6)]$$

$$H_{ij} = \int_{-h/2}^{h/2} C_{ijk} z^6 dz$$

$$= \int_{-h/2}^{Z_n} C_{ij2} z^6 dz + \int_{Z_n}^{h/2} C_{ij1} z^6 dz$$

$$= h^7[(C_{ij1} + C_{ij2})/896 + (C_{ij2} - C_{ij1})(Z_n^7/7)]$$

### References

- <sup>1</sup>Clark, S. K., "The Plane Elastic Characteristics of Cord-Rubber Laminates," *Textile Research Journal*, Vol. 33, April 1963, pp. 295-313.
- <sup>2</sup>Seldin, E. J., "Stress-Strain Properties of Polycrystalline Graphites in Tension and Compression at Room Temperature," *Carbon* 4, 1966, pp. 177-191.
- <sup>3</sup>Shapiro, G. S., "Deformation of Bodies with Different Tensile and Compressive Strengths (Stiffnesses)," *Mechanics of Solids*, Vol. 1, March-April 1966, pp. 85-86.
- <sup>4</sup>Kamiya, N., "Transverse Shear Effect in a Bimodulus Plate," *Nuclear Engineering and Design*, Vol. 32, July 1975, pp. 351-357.
- <sup>5</sup>Bert, C. W., "Classical Analysis of Laminated Bimodulus Composite-Material Plates," Univ. of Oklahoma, School of Aerospace, Mechanical and Nuclear Engineering, Contract 00014-78-C-0647, Rept. OU-AMNE-79-10A, July 1979.
- <sup>6</sup>Jones, R. M., "Buckling Circular Cylindrical Shells with Different Moduli in Tension and Compression," *AIAA Journal*, Vol. 9, Jan. 1971, pp. 53-61.
- <sup>7</sup>Reddy, J. N. and Bert, C. W., "Analyses of Plates Constructed of Fiber-Reinforced Bimodulus Materials," *ASME Mechanics of Bimodulus Materials*, Vol. 33, Dec. 1979, pp. 67-83.
- <sup>8</sup>Bert, C. W., Reddy, V. S., and Kincannon, S. K., "Deflection of Thin Rectangular Plates of Cross-Plyed Bimodulus Material," *Journal of Structural Mechanics*, Vol. 8, Aug. 1980, pp. 347-364.
- <sup>9</sup>Bert, C. W., Reddy, J. N., Reddy, V. S., and Chao, W. C., "Bending of Thick Rectangular Plates Laminated of Bimodulus Composite Materials," *AIAA Journal*, Vol. 19, Oct. 1981, pp. 1342-1349.
- <sup>10</sup>Reddy, J. N. and Chao, W. C., "Finite-Element Analysis of Laminated Bimodulus Plates," *Computers and Structures*, Vol. 12, No. 3, 1980, pp. 245-251.
- <sup>11</sup>Reddy, J. N. and Bert, C. W., "On the Behavior of Plates Laminated of Bimodulus Composite Materials," *Zeitschrift fuer Angewandte Mathematik und Mechanik*, Vol. 62, No. 3, 1982, pp. 213-219.
- <sup>12</sup>Brunelle, E. J. and Robertson, S. R., "Initially Stressed Mindlin Plates," *AIAA Journal*, Vol. 12, Aug. 1974, pp. 1036-1045.
- <sup>13</sup>Bert, C. W., Reddy, J. N., Chao, W. C., and Reddy, V. S., "Vibration of Thick Rectangular Plates of Bimodulus Composite Materials," *ASME Journal of Applied Mechanics*, Vol. 48, June 1981, pp. 371-376.
- <sup>14</sup>Bert, C. W. and Kumar, M., "Vibration of Cylindrical Shells of Bimodulus Composite Materials," *Journal of Sound and Vibration*, Vol. 81, March 1982, pp. 107-121.
- <sup>15</sup>Doong, J. L. and Chen, L. W., "Vibration of a Bimodulus Thick Plate," *Transactions of the ASME, Journal of Vibration, Acoustics, Stress, and Reliability in Design*, Vol. 107, Jan. 1985, pp. 92-97.
- <sup>16</sup>Dong, S. B. and Nelson, R. B., "On Natural Vibrations and Waves in Laminated Orthotropic Plates," *Journal of Applied Mechanics*, Vol. 39, Sept. 1972, pp. 739-745.
- <sup>17</sup>Srinivas, S., Joga Rao, C. V., and Rao, A. K., "An Exact Analysis for Vibration of Simply-Supported Homogeneous and Laminated Thick Rectangular Plates," *Journal of Sound and Vibration*, Vol. 12, June 1970, pp. 187-199.
- <sup>18</sup>Whitney, J. M. and Sun, C. T., "A Higher Order Theory for Extensional Motion of Laminated Composites," *Journal of Sound and Vibration*, Vol. 30, Sept. 1973, pp. 85-97.
- <sup>19</sup>Nelson, R. B. and Lorch, D. R., "A Refined Theory for Laminated Orthotropic Plates," *Journal of Applied Mechanics*, Vol. 41, March 1974, pp. 177-183.
- <sup>20</sup>Lo, K. H., Christensen, R. M., and Wu, E. M., "A High-Order Theory of Plate Deformation, Part I: Homogeneous Plates," *Journal of Applied Mechanics*, Vol. 44, Dec. 1977, pp. 663-668.
- <sup>21</sup>Bert, C. W., "A Critical Evaluation of New Plate Theories Applied to Laminated Composites," *Composite Structures*, Vol. 2, No. 4, 1984, pp. 329-347.
- <sup>22</sup>Doong, J. L., "Vibration and Stability of an Initially Stressed Thick Plate According to a High-Order Deformation Theory," *Journal of Sound and Vibration*, Vol. 113, March 1987, pp. 425-440.
- <sup>23</sup>Doong, J. L., Chen, T. J., and Chen, L. W., "Vibration and Stability of an Initially Stressed Laminated Plate Based on a Higher-Order Deformation Theory," *Composite Structures*, Vol. 7, No. 4, 1987, pp. 285-309.
- <sup>24</sup>Brunelle, E. J. and Robertson, S. R., "Vibrations of an Initially Stressed Thick Plate," *Journal of Sound and Vibration*, Vol. 45, April 1976, pp. 405-416.
- <sup>25</sup>Jones, R. M., *Mechanics of Composite Materials*, McGraw-Hill, New York, 1975.